Carbohydrate Polymers 117 (2015) 585–591

Contents lists available at ScienceDirect

Carbohydrate Polymers

journal homepage: www.elsevier.com/locate/carbpol

The hygroscopic power of amorphous cellulose: A modeling study

Karim Mazeau*

Univ. Grenoble Alpes, CNRS CERMAV, F-38000 Grenoble, France

ARTICLE INFO

Article history:
Received 25 July 2014
Received in revised form
23 September 2014
Accepted 26 September 2014
Available online 15 October 2014

Keywords:
Amorphous cellulose
Glass transition
Water diffusion
Hydration
Swelling
Hygroexpansion

ABSTRACT

The relationship between cellulose and water was studied by building dense amorphous cellulose models and subjecting them to increasing moisture contents. When starting from completely dry cellulose, the first diffused water molecules were essentially individualized and hydrogen bonded exclusively to the O6 and O2 hydroxyl groups of cellulose. Upon continued hydration increase, the hydroxyl at O3 and then the acetal oxygens of cellulose also started to attract the upcoming water molecules, which were no longer isolated. They progressively became aggregated, first into clusters and then at high hydration content, into continuous capillary channels.

A benefit of this study was to allow predicting a number of physical parameters of amorphous cellulose and their variation under hydration. With some parameters, the calculated values matched rather well the experimental literature determinations. This was the case for the hydration dependence of Tg, the stereoselectivity of the cellulose oxygen atoms for water molecules, together with the diffusion coefficients of water into cellulose. An estimate of the hygro-expansion of amorphous cellulose was provided.

1. Introduction

The hydrophilic character of cellulose and more generally the interactions of water and cellulose have a fundamental importance for the physico-chemical properties, the manufacturing and the end-uses of cellulose-based materials. Due to the importance of the relationship between water and cellulose, myriads of reports – well summarized in several reviews and conference proceedings (Engelund, Thygesen, Svensson, & Hill, 2013; Hatakeyama & Hatakeyama, 1998; Samyn, 2013) have been published on this topic. The wetting and de-wetting processes of cellulose are generally characterized by their water sorption isotherms, (Despond, Espuche, Cartier, & Domard, 2005; Kocherbitov, Ulvenlund, Kober, Jarring, & Arnebrant, 2008; Okubayashi, Griesser, & Bechtold, 2004; Sun et al., 2010) whose sigmoidal shape suggests that the water uptake occurs in three steps (Ebrahimzadeh & McQueen, 1998). The rapid initial uptake expresses the extreme hygroscopicity of dry cellulose, which reflects tight interactions between cellulose and water. It is generally admitted that the first water molecules adsorb on the polar accessible groups of cellulose as they are logically suspected to be the most favorable adsorption sites (Berthold, Rinaudo, & Salmen, 1996). This first water, which is undetected by scanning calorimetry, is consequently called non-freezing water. In the mid-range of hydration, the linear and very slow water uptake is interpreted as the formation of water clusters. In this process, the most favorable sites which were occupied by the first water molecules, are followed by additional ones, leading to their aggregation into primary clusters (Grigoriew & Chmielewski, 1998) whose average size is in the range of 3–4 molecules (Despond et al., 2005). These water molecules, identified as freezing-bound water, can be detected by DSC but display melting temperatures lower than 0 °C. The final steep increase of the isotherm is due to the capillary condensation of the water molecules. Such capillary water, which melts at 0 °C is called free water.

At the atomic scale, the adsorption of water in cellulosic materials is a very complex process due to the hierarchical organization of the material and the coexistence of amorphous and crystalline phases. As cellulose crystals are impermeable to hydration, the water molecules can adsorb only at their surfaces and there is no influence of water on the properties of the cellulose crystals. On the other hand, water, which is free to penetrate the amorphous domains, strongly affects the physico-chemical properties of such a phase (Mihranyan, Llagostera, Karmhag, Stromme, & Ek, 2004; Mohan et al., 2012; Stromme, Mihranyan, Ek, & Niklasson, 2003). All the key interactions between water and cellulose are thus concentrated essentially within the cellulose amorphous phase (Princi, Vicini, Pedemonte, Arrighi, & McEwen, 2005).

* Tel.: +330476037602; fax: +330476547203..
E-mail address: karim.mazeau@cermav.cnrs.fr

http://dx.doi.org/10.1016/j.carbpol.2014.09.095
0144-8617/

Completely amorphous samples of cellulose are not natural but they can be produced following different methods (Ciolacu, Ciolacu, & Popa, 2011), including ball milling (Hermans & Weidinger, 1946; Shimura, Nishioka, Kano, Koda, & Nishio, 2014; Stubicar et al., 1998), deacetylation of cellulose acetate under non aqueous conditions (Manley, 1963) and regeneration of cellulose solutions into non aqueous media (Atalla, Ellis, & Schroeder, 1984; Schroeder, Gentile, & Atalla, 1986). Whereas many of these amorphous celluloses will readily recrystallize in water (Ciesla, Rahier, & Zakrzewska-Trznadel, 2004; Hatakeyama & Hatakeyama, 1981, 1998; Hatakeyama, Nakamura, & Hatakeyama, 2000; Kimura, Hatakeyama, & Nakano, 1974; Paes et al., 2010), some specimens remain amorphous under hydrated conditions (Isogai & Atalla, 1991; Isogai, Akishima, Onabe, Usuda, & Atalla, 1989) and among these, some of them display remarkable swelling properties (Kontturi et al., 2011). Producing fully amorphous cellulose is attracting a substantial interest as it is considered as being a new promising material (Schurz, 2003).

The structure and hydration behavior of amorphous cellulose are difficult to access experimentally. The data from experiments of non-ordered materials are generally of low resolution and this is the case for amorphous cellulose (Avolio et al., 2012; Mori et al., 2012). Moreover, the samples are far from perfect, as amorphous cellulose may contain a small amount of crystalline domains (Avolio et al., 2012) and a variable amount of water (Princi et al., 2005). It is consequently difficult to extract from the experimental data a detailed understanding of the relationship between amorphous cellulose and water. In this context, modeling appears to be a choice tool by providing a library of modeled hydrated structures. In a preceding report, we have modeled the static structural parameters of anhydrous amorphous bulk cellulose (Mazeau & Heux, 2003). In this study, we have considered six hydration states, ranging from 0.8% to 36.4% of water (w/w) and determined their main characteristics. These models, which compared favorably with the data derived from experimental details, allow us to propose an improved overall view of the swelling mechanism of amorphous cellulose with water.

2. Experimental

2.1. Computational details

In this study, we have used the modeling softwares Cerius2 and Material Studio (Accelrys Inc., San Diego, CA, USA); all calculations were achieved at the Centre d'Expérimentation et de Calcul Intensif CECIC, Grenoble, France. Energy calculations were performed using the PCFF forcefield (Maple, Dinur, & Hagler, 1988). Partial charges on atoms were calculated by the charge equilibration method (Rappé & Goddard, 1991). A simple three-point charge model was used for the water molecules (Berendsen, Postma, van Gunsteren, & Hermans, 1981).

Energy minimization was performed by the steepest descent method and then by the conjugated gradient method. The convergence criterion was a root-mean-square (rms) force of less than 0.1 kcal mol^{-1} $Å^{-1}$. Molecular dynamics was then used in the NVT and NPT ensembles, employing the standard Verlet algorithm (Verlet, 1967) for the integration of the Newton's laws of motion with a time step of 0.001 ps. Molecular dynamics runs were initiated by assigning an initial velocity to the atoms according to a Boltzmann distribution at 2*T*, *T* being the target temperature. The atom velocities were quickly scaled down so that the final atom temperature was *T*. The total external pressure was maintained at 1 atm and a Hoover algorithm (Evans & Holian, 1985) was used to keep the cell temperature constant during the run. Most simulations were performed at 300 K and lasted 1 ns in order to define the structural characteristics of the models, but some of them were extended to 5 ns in order to account for the mobility of the water molecules. Similar simulations were performed at different temperatures in order to estimate the glass transition temperature.

2.2. Generation and relaxation of the models

The generation and relaxation protocols for the modeling of amorphous solids of cellulose are fully described elsewhere (Mazeau & Heux, 2003). In short, a cube subjected to periodic boundary conditions following the three dimensions was first defined. This cube was then filled by two chains of cellulose, each defined by 40 anhydroglucosyl units (AGU) and organized in a coil conformation, with each chain generated residue by residue, using a Monte–Carlo protocol. A given quantity of water molecules was then added into the empty domains of the cell (see Table 1). The different systems considered contained a variable number of water molecules (0–263). Each system, with its water content is represented by five microstructures. The results were perfectly reproducible among the five microstructures.

Once generated, the system was then relaxed to a mechanical equilibrium. The relaxation was achieved by using successive steps of energy minimization and molecular dynamics experiments first in the NVT ensemble at elevated temperatures and then in the more realistic NPT ensemble at a reasonable temperature and at atmospheric pressure. The first 100–200 ps of the NPT, in which a given property (density for example) may vary with time, were used to relax and equilibrate the models. The part of the trajectory, where a given property remained stable, was used to estimate its average characteristics.

2.3. Characteristics of the computed models

The water content by mass is defined by:

$$\%W_{\mathrm{H}}\mathrm{H_2O} = 100\left(\frac{W_{\mathrm{H}} - W_{\mathrm{D}}}{W_{\mathrm{D}}}\right)$$

where W_{H} is the weight of the hydrated sample and W_{D} is the dry weight.

The volumetric swelling is defined by:

$$\%\Delta V = 100\left(\frac{V_{\mathrm{H}} - V_{\mathrm{D}}}{V_{\mathrm{D}}}\right)$$

where V_{H} and V_{D} are the volumes of the hydrated and dry samples, respectively.

The hygroexpansion coefficient, β, corresponds to the volumetric change divided by the moisture change of the sample, both expressed in % (Pulkkinen, Fiskari, & Alopaeus, 2009b): it is calculated with the following expression:

$$\beta = \frac{\Delta V}{\Delta W}$$

where *W* is the mass of water.

The mobility of the water molecules can be estimated from the Einstein relation:

$$D = \frac{1}{6}\lim\frac{d}{dt}[r(t) - r(o)]^2$$

where *D* is the diffusion coefficient. The mean square displacement (MSD) of the water molecules was taken as an ensemble average over all water molecules and all time origins.

3. Results and discussion

We have considered six hydration states of amorphous cellulose covering the whole range of moisture observed in the adsorption isotherms, ranging from the pure dry state (0% H_2O) up to a wet

Table 1
Average characteristics of the models. Volumes in Å^3, densities in g cm^{-3}, voids in Å^3, *D*: diffusion coefficients of the water molecules in m^2 s^{-1} 10^{-11}.

nH_2O	0	6	33	66	131	197	263
%H_2O (w/w)	0	0.83	4.57	9.14	18.14	27.29	36.43
Volume	18429 ± 300	19454 ± 248	19478 ± 235	20008 ± 166	21919 ± 220	23943 ± 328	25896 ± 155
Density	1.188 ± 0.023	1.192 ± 0.017	1.197 ± 0.009	1.205 ± 0.006	1.202 ± 0.010	1.187 ± 0.013	1.179 ± 0.003
Voids	0.53 ± 0.19	0.71 ± 0.20	1.24 ± 0.21	1.57 ± 0.20	2.75 ± 0.22	4.24 ± 0.27	5.81 ± 0.21
D	–	1.08	0.602	0.320	0.130	0.170	0.072

state having 40% in weight of water molecules. Note that with respect to one AGU, 1 and 2 water molecules correspond respectively to 12% and 24% of water.

3.1. Bulk properties

The average predicted densities and volumes at equilibrium of each system are given in Table 1. All the densities were around 1.2 g cm^{-3}, i.e. 20% lower than that of the crystalline phase, which is a reasonable value (Mazeau & Heux, 2003).

The equilibrated total volumes and void volumes of the different systems, reported in Table 1 can be used to characterize the volumetric swelling resulting from the water uptake (Fig. 1) and the hygro-expansion coefficient of amorphous cellulose. During water uptake, from 0% to 36%, the total volume of the model increased linearly in an isotropic manner, yielding a hygro-expansion coefficient β calculated at 0.0097%.

With cellulose-based products, such as pulp and paper, the hygro-expansion parameter is a key indicator that needs to be controlled for maintaining an acceptable dimensional stability in case of moistening. In the present work, a value of 0.0097% was obtained for this parameter. This calculated value is far lower than the measured values ranging from around 0.02% to 0.21%, as quoted for the hygro-expansion of paper handsheets (Lee, Pawlak, & Heitmann, 2012; Pulkkinen, Fiskari, & Alopaeus, 2009a). For such products the high value does not seem to be connected to the amorphous cellulosic component of the product, but rather to the swelling propensity of the hemicelluloses, that are present in the specimens. Additionally, the specific ultrastructural organization of the cellulose microfibrils within the fiber cell walls, which is not present in our model of amorphous cellulose, is also given as another reason for a high hygro-expansion figure of paper products (Pulkkinen et al., 2009a, 2009b).

3.2. Distribution of the water molecules within the volumes

The water molecules inside the amorphous cellulose matrix can be individual, i.e. each water molecule isolated from the other water molecules, or aggregated. To distinguish these two classes of water molecules, we have analyzed their distances throughout the trajectories. Two water molecules were considered bounded if their distance was lower than 4 Å. The water molecules, which spent more than 80% of the total time far from the other water molecules, were considered isolated. Conversely, the water molecules, which spent more than 80% of the time bounded to other water molecules, were considered to belong to an aggregate.

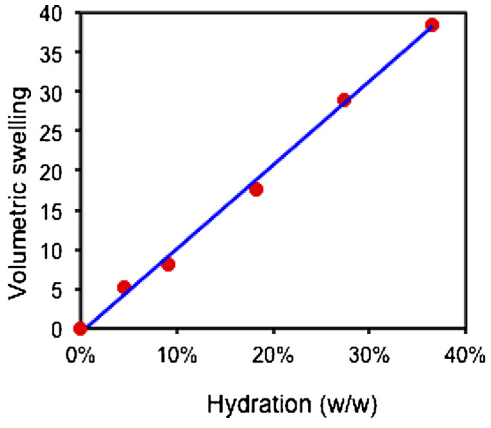

Fig. 1. Variation of the predicted volumes as a function of moisture content.

To illustrate the organization of the water molecules within the model, Fig. 2 shows only the water molecules within the periodic limit of the models, whereas Fig. 3A–C gives the selected radial distribution functions (RDF) specifically calculated between the oxygen atoms of the water molecules. The peak at 3 Å in oxygen-to-oxygen RDF is particularly important, as it is typical of hydrogen bonding. In this context it provides an evidence for the aggregated state of the water molecules.

At a moisture content of 0.8%, the water molecules were isolated from the other water molecules, a feature easily perceptible in Fig. 2. This was confirmed in Fig. 3A, which showed two peaks at 5.5 Å and 7 Å and the absence of peak at 3 Å.

At 4.6% moisture, small aggregates of water molecules occurred, which were clearly visible in the model and in the water-to-water RDF. The water clusters contained in average between 2 and 5 molecules and there still existed an amount of isolated water molecules that could not be detected from the RDF measurements.

At 9.1% moisture, there were large aggregates of water (Fig. 2). When the amount of water further increases, at 18%, one observes strands of water occupying channels between the cellulose chains. At this stage, the percolated network of water molecules is consistent with the phenomenon of capillary condensation.

3.3. Preferred hydration sites on cellulose

Fig. 3D–F shows the RDF calculated between the oxygen atoms of cellulose and those of water molecules, identified as water to cellulose RDF. These RDF revealed the preferred interaction sites of water on cellulose. Note that several hydrophilic moieties on each repeat unit of cellulose can interact with water, namely two secondary hydroxyl groups at O2 and O3, a single primary hydroxyl group at O6, together with the two acetal oxygen atoms O5 and O4 (Fig. 4).

At 0.8% of moisture (Fig. 3D), the water molecules interacted exclusively with cellulose: the water to cellulose RDF revealed that the water molecules formed hydrogen bonds quasi exclusively with the hydroxyl groups of cellulose at O6 and O2. The preference of interaction was O6 > O2 > > > O3, O4, O5.

At 4.6% of moisture (Fig. 3E), the water to cellulose RDF revealed a marked contribution of the hydroxyl group at O3 in its interaction with the water molecules, in addition to those at O2 and O6 detected at 0.8%. At this hydration level, the ranking preference was O6 > O2 = O3 > > > O4, O5.

At 18% of moisture (Fig. 3F), the water to cellulose RDF revealed that the acetal oxygens became substantially involved in the interactions with water and the corresponding ranking was: O6 = O2 = O3 > O4 = O5.

The predicted regioselective adsorption of water on amorphous cellulose can be compared to the reported regioselectivity

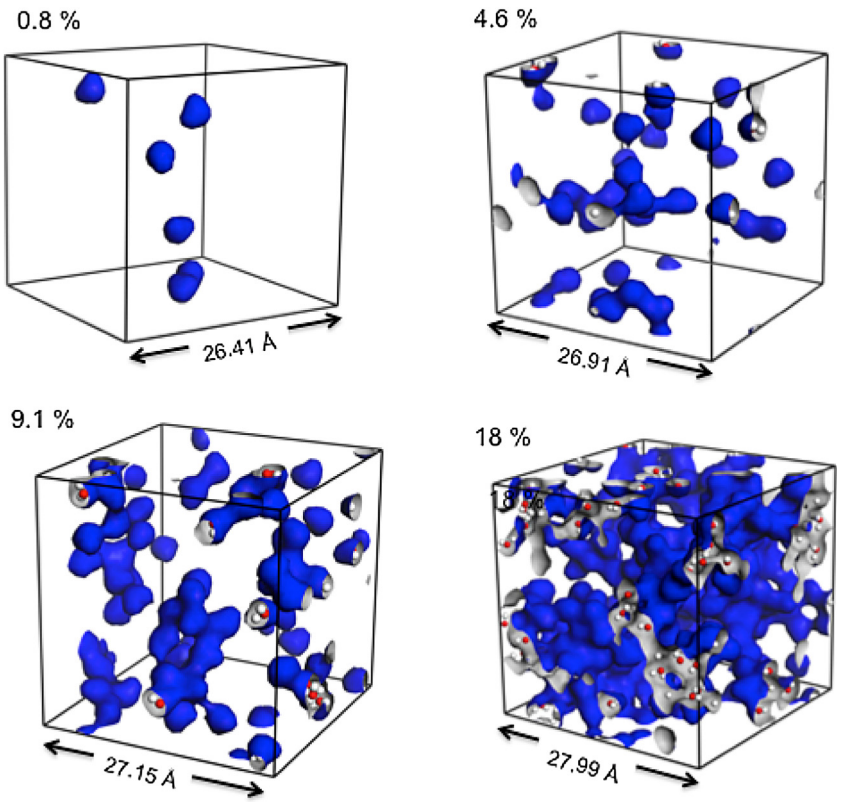

Fig. 2. Distribution of the water molecules in the models at different moisture contents. The dimensions of the periodic cells are indicated.

of cellulose subjected to various derivatization reactions. With heterogeneous reactions and using semi crystalline cellulose, the O3 is not easily accessible to any derivatization due to its engagement in an intra-molecular hydrogen bond with the O5 of the next AGU unit (Rowland, Roberts, & Wade, 1969). Regarding the selectivity of the oxygen at C2 versus the one at C6, the bulkiness of the reagent needs to be considered, the most bulky reagents reacting with the C6 exclusively (Klemm, Philipp, Heinze, Heinze, & Wagenknecht, 1998), whereas in other cases, the reactivity at O2 exceeds that at O6 (Rowland et al., 1969; Salmi, Damlin, Mikkola, & Kangas, 2011). When considering the derivatization of cellulose in homogeneous phases, the C6 position is generally the preferred site of reaction,

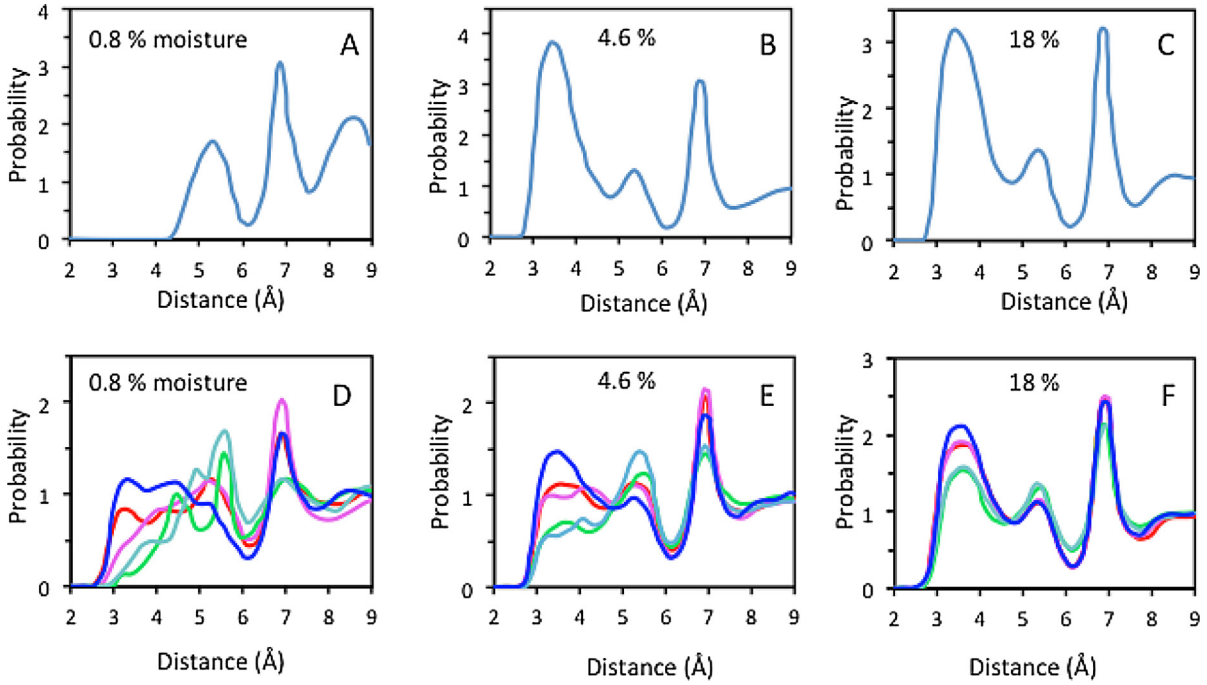

Fig. 3. Radial distribution functions (RDF). 3A–3C. RDF of the water-to-water interactions at various hydration content. 3D–3F. Identical to 3A–3C, but water to cellulose hydroxyl interactions: blue Ow-O6, red Ow-O2, rose Ow-O3, green Ow-O4, turquoise Ow-O5.

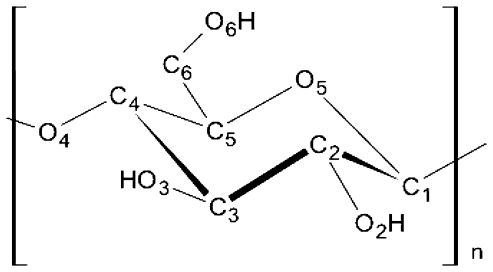

Fig. 4. Numbering system for oxygen and carbon atoms in the anhydro-glucose unit of cellulose.

but the reactivity at C2 and C3 may depend on the reagent. Taking into account these experimental facts and comparing them with our modeling regioselectivity, it is not possible to draw a definitive concordance, except for the selectivity of C6, which appears to be preferred, both in our conditions of low water content and in the actual homogeneous derivatization.

3.4. Mobility of the water molecules

Fig. 5 shows the displacement of one water molecule, randomly selected, from its origin in the model at 0.8% of moisture. The water molecule moved within the cellulose matrix from one hole to the other by jumps, but during some time, it stayed at certain position with continuous fluctuation, thus leading to an irregular behavior throughout the simulation. The mechanism by which the water molecules are susceptible to jump from one hole to the next takes its origin in the fluctuations of the cellulose matrix, with the consequence of transient channel openings between holes.

The mobility of the water molecules can be deduced from the Einstein relation. Fig. 6 shows the average variation of the mean square displacement (MSD) of the water molecules as a function of time for two water contents, at 4.6% and 9.1% of moisture, respectively. The linearity of the MSD curves was satisfactory and the diffusion coefficients of water were consequently estimated from the linear portion of the curves. The estimated diffusion coefficients of water in an amorphous cellulose matrix at different moisture contents are given in Table 1.

While tightly bound to cellulose, the isolated water molecules are far from immobile, their predicted diffusion coefficients were estimated at 1.1×10^{-11} m^2 s^{-1}.

The mobility of the water molecules surprisingly decreased when moisture content increased (Fig. 7). The clustered water molecules showed diffusion coefficients of one order of magnitude lower than those obtained for the dispersed water molecules. The water molecules in the aggregates moved together and behaved as a single particle. Such effect has been documented in synthetic hydrophilic polymers (Williams, Hopfenberg, & Stannett, 1969).

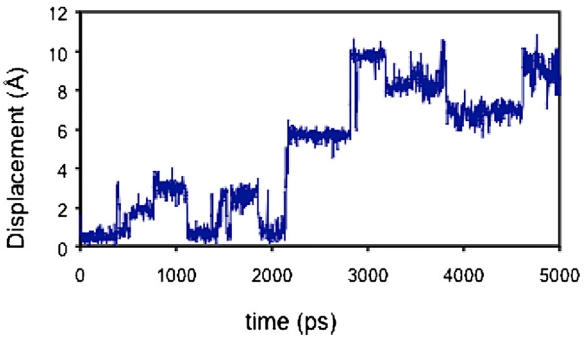

Fig. 5. Displacement from its origin of a randomly selected single water molecule as a function of time for the cellulosic model at 0.8% of moisture.

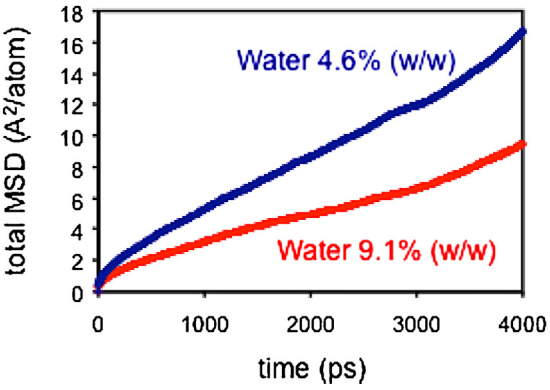

Fig. 6. Mean square displacements of the water molecules. Blue: model hydrated at 4.6%, red: model hydrated at 9.1%.

The decrease in diffusion of the water molecules reached however a plateau when 18% of water was reached. In this study, this may be the point indicating the boundary between the "non freezing" and "freezing" water.

The diffusion coefficient, which was calculated at 1.1×10^{-11} m^2 s^{-1} for 0.8% hydration, was divided by three at 9% and by close to 10% at 18% hydration, beyond which it stayed more or less constant at this low value, until 40% hydration, the maximum water content considered in this study. These values are not to far from $6.7 \pm 2.2 \times 10^{-11}$ m^2 s^{-1}, resulting from pulsed field gradient NMR data on hydrated cotton linters (Newling & Batchelor, 2003).

3.5. Volume temperature behavior and prediction of the Tg of amorphous cellulose

Fig. 8 shows the temperature dependence of the specific volume of the dry model and of the model hydrated at 4.6%. The same trend was observed for the two systems: the specific volumes showed two linear variations as a function of temperature, with a lower thermal expansivity for the low temperature side. The inflexion point of the low and high temperature branches corresponds to the glass transition temperature of the system. Tg of dry amorphous cellulose was consequently estimated at 630 K, and that of the model hydrated at 4.6% was shifted toward a lower temperature, at around 520 K.

The measured Tg$_s$ of cellulose range from 478 K to 512 K (Alfthan, De Ruvo, & Brown, 1973; Batzer & Kreibich, 1981; Paes et al., 2010; Salmen & Back, 1977; Szczesniak, Rachocki, & Tritt-Goc, 2008). The calculated Tg is higher than the experimental values, but this discrepancy is well documented and may have several origins (Barrat, Baschnagel, & Lyulin, 2010). The heating/cooling

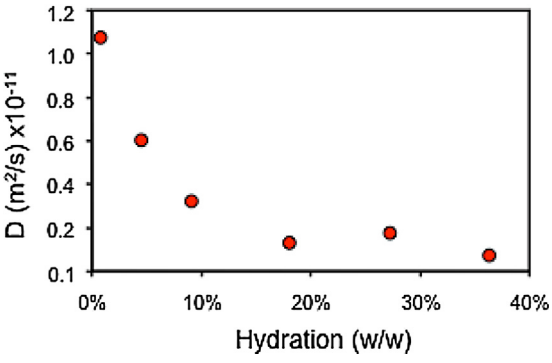

Fig. 7. Variation of the predicted diffusion coefficients of the water molecules as a function of moisture content.

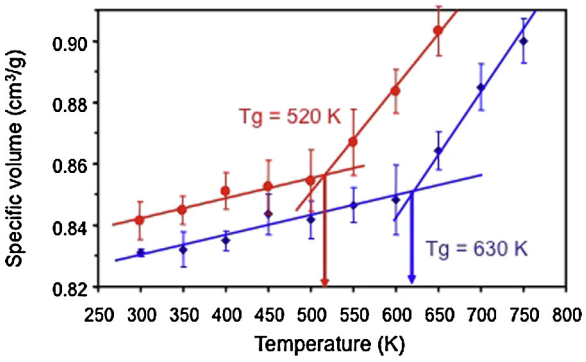

Fig. 8. Variation of the specific volume with temperature. Blue: dry model, red: model hydrated at 4.6%.

rates have a strong influence on Tg since it depends on kinetic phenomenon. Typical rates for measuring Tg are of the order of 10 K/min, whereas the modeling uses considerably faster rates, of the order of 10^{12} K/min, thus causing a shift of calculated Tg toward higher temperatures. In addition, Tg also depends on the polymer weight and the models are made of very small chains compared to what is used in experimentations. In the experimental determinations, the crystallinity of the samples may also be an obstacle for the determination of Tg and thus its values may be slightly different for samples of high crystallinity as opposed to those where the amorphous phase is important. Even if the calculated Tg is systematically higher than its experimental counterparts, it is interesting to see that the modeled spectacular drop of 110 degrees in Tg, when as little as 4.6% of water is added to dry amorphous cellulose, matches reasonably well the Tg drop mentioned in several experimental studies when water is added to dry cellulose (Batzer & Kreibich, 1981; Paes et al., 2010; Szczesniak et al., 2008).

4. Concluding remarks

The preparation of bulk cellulose samples entirely consisting of amorphous phase, devoid of any crystalline or paracrystalline phase and stable under anhydrous or hydrated conditions has been rather difficult or even impossible so far. If such samples could be produced in sufficient quantity, they are expected to be promising new materials endowed with a number of interesting properties (Schurz, 2003). In an exciting breakthrough, the preparation of 20 μm thick films of amorphous cellulose has been implemented recently. The samples, which result from the gas phase de-silylation of spin-coated trimethylsilyl cellulose films, meet the requirements of a stable and entirely amorphous phase of cellulose (Holmberg et al., 1997; Kontturi, Tammelin, & Osterberg, 2006; Kontturi et al., 2011). Preliminary results have shown that, these films displayed remarkable properties, such as swelling reversibility in aqueous environment, ease of dissolution into dilute alkali and high susceptibility toward endoglucanase digestion (Kontturi et al., 2011; Suchy et al., 2011). When dealing with these films, whose ultrastructure seems to meet that of our model, it would be most interesting to measure the series of physical properties that have been mentioned in this report and to follow the evolution of these properties during hydration experiments. Confronting such measurements with our calculated values should bring further proof of our model validity.

Acknowledgments

The help of H. Chanzy for valuable comments during the writing of this manuscript is acknowledged.

References

Alfthan, E., De Ruvo, A., & Brown, W. (1973). Glass transition temperatures of oligosaccharides. *Polymer*, *14*(7), 329–330.
Atalla, R. H., Ellis, J. D., & Schroeder, L. R. (1984). Some effects of elevated temperatures on the structure of cellulose and its transformation. *Journal of Wood Chemistry and Technology*, *4*(4), 465–482.
Avolio, R., Bonadies, I., Capitani, D., Errico, M. E., Gentile, G., & Avella, M. (2012). A multi-technique approach to assess the effect of ball milling on cellulose. *Carbohydrate Polymers*, *87*, 265–273.
Barrat, J.-L., Baschnagel, J., & Lyulin, A. (2010). Molecular dynamics simulations of glassy polymers. *Soft Matter*, *6*(15), 3430–3446.
Batzer, H., & Kreibich, U. T. (1981). Influence of water on thermal transitions in natural polymers and synthetic polyamides. *Polymer Bulletin*, *5*, 585–590.
Berendsen, H. J. C., Postma, J. P. M., van Gunsteren, W. F., & Hermans, J. (1981). Interaction models for water in relation to protein hydration. In B. Pullman (Ed.), *Intermolecular forces* (pp. 331–342). Dordrecht: Reidel Pub Co.
Berthold, J., Rinaudo, M., & Salmen, L. (1996). Association of water to polar groups; estimations by an adsorption model for ligno-cellulosic materials. *Colloids and Surfaces A*, *112*(2/3), 117–129.
Ciesla, K., Rahier, H., & Zakrzewska-Trznadel, G. (2004). Interaction of water with the regenerated cellulose membrane studied by DSC. *Journal of Thermal Analysis and Calorimetry*, *77*(1), 279–293.
Ciolacu, D., Ciolacu, F., & Popa, V. I. (2011). Amorphous cellulose—Structure and characterization. *Cellulose Chemistry and Technology*, *45*(1–2), 13–21.
Despond, S., Espuche, E., Cartier, N., & Domard, A. (2005). Hydration mechanism of polysaccharides: A comparative study. *Journal of Polymer Science Part B Polymer Physics*, *43*(1), 48–58.
Ebrahimzadeh, P. R., & McQueen, D. H. (1998). A model of the dynamic mechanical responses of wood, paper and some polymers to moisture changes. *The Journal of Materials Science*, *33*(5), 1201–1209.
Engelund, E. T., Thygesen, L. G., Svensson, S., & Hill, C. A. S. (2013). A critical discussion of the physics of wood–water interactions. *Wood Science and Technology*, *47*, 141–161.
Evans, D. J., & Holian, B. L. (1985). The Nose–Hoover thermostat. *The Journal of Chemical Physics*, *83*(8), 4069–4074.
Grigoriew, H., & Chmielewski, A. G. (1998). Capabilities of X-ray methods in studies of processes of permeation through dense membranes. *The Journal of Membrane Science*, *142*(1), 87–95.
Hatakeyama, H., & Hatakeyama, T. (1981). Structural change of amorphous cellulose by water- and heat-treatment. *Makromolekulare Chemie*, *182*(6), 1655–1668.
Hatakeyama, H., & Hatakeyama, T. (1998). Interaction between water and hydrophilic polymers. *Thermochimica Acta*, *308*(1–2), 3–22.
Hatakeyama, T., Nakamura, K., & Hatakeyama, H. (2000). Vaporization of bound water associated with cellulose fibres. *Thermochimica Acta*, *352–353*, 233–239.
Hermans, P. H., & Weidinger, A. (1946). Recrystallization of amorphous cellulose. *The Journal of the American Chemical Society*, *68*, 2547–2552.
Holmberg, M., Berg, J., Stemme, S., Oedberg, L., Rasmusson, J., & Claesson, P. (1997). Surface force studies of Langmuir–Blodgett cellulose films. *The Journal of Colloid and Interface Science*, *186*(2), 369–381.
Isogai, A., Akishima, Y., Onabe, F., Usuda, M., & Atalla, R. H. (1989). Preparation and characterisation of stable amorphous cellulose. In G. O. Phillips, J. F. Kennedy, & P. A. Williams (Eds.), *Cellulose, structural and functional aspects* (pp. 105–110). Chichester Ellis Horwood, Ltd.
Isogai, A., & Atalla, R. H. (1991). Amorphous celluloses stable in aqueous media: Regeneration from SO_2-amine solvent systems. *Journal of Polymer Science Part A: Polymer Chemistry*, *29*(1), 113–119.
Kimura, M., Hatakeyama, T., & Nakano, J. (1974). DSC study on recrystallization of amorphous cellulose with water. *The Journal of Applied Polymer Science*, *18*(10), 3069–3076.
Klemm, D., Philipp, B., Heinze, T., Heinze, U., & Wagenknecht, W. (1998). *Comprehensive cellulose chemistry. Functionalization of cellulose* (2) Weinheim: Wiley-VCH Verlag GmbH.
Kocherbitov, V., Ulvenlund, S., Kober, M., Jarring, K., & Arnebrant, T. (2008). Hydration of microcrystalline cellulose and milled cellulose studied by sorption calorimetry. *Journal of Physical Chemistry B*, *112*(12), 3728–3734.
Kontturi, E., Suchy, M., Penttila, P., Jean, B., Pirkkalainen, K., Torkkeli, M., et al. (2011). Amorphous characteristics of an ultrathin cellulose film. *Biomacromolecules*, *12*(3), 770–777.
Kontturi, E., Tammelin, T., & Osterberg, M. (2006). Cellulose-model films and the fundamental approach. *Chemical Society Reviews*, *35*(12), 1287–1304.
Lee, J. M., Pawlak, J. J., & Heitmann, J. A. (2012). Dimensional and hygroexpansive behaviors of cellulose microfibrils (MFs) from kraft pulp-based fibers as a function of relative humidity. *Holzforschung*, *66*, 1001–1008.
Manley, R. S. J. (1963). Hydrolysis of cellulose triacetate crystals. *Journal of Polymer Science Part A*, *1*, 1893–1899.
Maple, J. R., Dinur, U., & Hagler, A. T. (1988). Derivation of force fields for molecular mechanics and dynamics from ab initio energy surfaces. *Proceedings of the National Academy of Sciences United States of America*, *85*, 5350–5354.
Mazeau, K., & Heux, L. (2003). Molecular dynamics simulations of bulk native crystalline and amorphous structures of cellulose. *The Journal of Physical Chemistry B*, *107*(10), 2394–2403.
Mihranyan, A., Llagostera, A. P., Karmhag, R., Stromme, M., & Ek, R. (2004). Moisture sorption by cellulose powders of varying crystallinity. *International Journal of Pharmaceutics*, *269*(2), 433–442.

Mohan, T., Spirk, S., Kargl, R., Doliska, A., Vesel, A., Salzmann, I., et al. (2012). Exploring the rearrangement of amorphous cellulose model thin films upon heat treatment. *Soft Matter*, *8*, 9807–9815.

Mori, T., Chikayama, E., Tsuboi, Y., Ishida, N., Shisa, N., Noritake, Y., et al. (2012). Exploring the conformational space of amorphous cellulose using NMR chemical shifts. *Carbohydrate Polymers*, *90*(3), 1197–1203.

Newling, B., & Batchelor, S. N. (2003). Pulsed field gradient NMR study of the diffusion of H_2O and polyethylene glycol polymers in the supramolecular structure of wet cotton. *The Journal of Physical Chemistry B*, *107*(45), 12391–12397.

Okubayashi, S., Griesser, U. J., & Bechtold, T. (2004). A kinetic study of moisture sorption and desorption on lyocell fibers. *Carbohydrate Polymers*, *58*(3), 293–299.

Paes, S. S., Sun, S., MacNaughtan, W., Ibbett, R., Ganster, J., Foster, T. J., et al. (2010). The glass transition and crystallization of ball milled cellulose. *Cellulose*, *17*(4), 693–709.

Princi, E., Vicini, S., Pedemonte, E., Arrighi, V., & McEwen, I. (2005). Thermal characterization of cellulose based materials. Investigation of water content. *Journal of Thermal Analysis and Calorimetry*, *80*, 369–373.

Pulkkinen, I., Fiskari, J., & Alopaeus, V. (2009a). CPMAS ^{13}C NMR analysis of fully bleached eucalypt pulp samples: Links to handsheet hygroexpansivity and strength properties. *Journal of Applied Sciences*, *9*(22), 3991–3998.

Pulkkinen, I., Fiskari, J., & Alopaeus, V. (2009b). The effect of hardwood fiber morphology on the hygroexpansivity of paper. *BioResources*, *4*(1), 126–141.

Rappé, A. K., & Goddard, W. A., III. (1991). Charge equilibration for molecular dynamics simulations. *The Journal of Physical Chemistry*, *95*(8), 3358–3363.

Rowland, S. P., Roberts, E. J., & Wade, C. P. (1969). Selective accessibilities of hydroxyl groups in the microstructure of cotton cellulose. *Textile Research Journal*, *39*, 530–542.

Salmen, N. L., & Back, E. L. (1977). The influence of water on the glass transition temperature of cellulose. *Tappi*, *60*(12), 137–140.

Salmi, T., Damlin, P., Mikkola, J.-P., & Kangas, M. (2011). Modelling and experimental verification of cellulose substitution kinetics. *Chemical Engineering Science*, *66*, 171–182.

Samyn, P. (2013). Wetting and hydrophobic modification of cellulose surfaces for paper applications. *Journal of Materials Science*, *48*, 6455–6498.

Schroeder, L. R., Gentile, V. M., & Atalla, R. H. (1986). Nondegradative preparation of amorphous cellulose. *Journal of Wood Chemistry and Technology*, *6*(1), 1–14.

Schurz, J. (2003). Amorphous cellulose. A new, renewable raw material? *Cellulose Chemistry and Technology*, *37*(1–2), 3–5.

Shimura, R., Nishioka, A., Kano, I., Koda, T., & Nishio, T. (2014). Novel method for producing amorphous cellulose only by milling. *Carbohydrate Polymers*, *102*, 645–648.

Stromme, M., Mihranyan, A., Ek, R., & Niklasson, G. A. (2003). Fractal dimension of cellulose powders analyzed by multilayer BET adsorption of water and nitrogen. *The Journal of Physical Chemistry B*, *107*(51), 14378–14382.

Stubicar, N., Smit, I., Stubicar, M., Tonejc, A., Janosi, A., Schurz, J., et al. (1998). An X-ray diffraction study of the crystalline to amorphous phase change in cellulose during high-energy dry ball milling. *Holzforschung*, *52*(5), 455–458.

Suchy, M., Linder, M. B., Tammelin, T., Campbell, J. M., Vuorinen, T., & Kontturi, E. (2011). Quantitative assessment of the enzymatic degradation of amorphous cellulose by using a quartz crystal microbalance with dissipation monitoring. *Langmuir*, *27*(14), 8819–8828.

Sun, S., Mitchell, J. R., MacNaughtan, W., Foster, T. J., Harabagiu, V., Song, Y., et al. (2010). Comparison of the mechanical properties of cellulose and starch films. *Biomacromolecules*, *11*, 126–132.

Szczesniak, L., Rachocki, A., & Tritt-Goc, J. (2008). Glass transition temperature and thermal decomposition of cellulose powder. *Cellulose*, *15*(3), 445–451.

Verlet, L. (1967). Computer experiments on classical fluids. I. Thermodynamical properties of Lennard-Jones molecules. *Physical Review*, *159*(1), 98–103.

Williams, J. L., Hopfenberg, H. B., & Stannett, V. (1969). Water transport and clustering in poly(vinyl chloride), poly(oxymethlene), and other polymers. *Journal of Macromolecular Science, Part B. Physics*, *3*(4), 711–725.